Self-sustaining charging of identical colliding particles

Theo Siu, Jake Cotton, Gregory Mattson, and Troy Shinbrot[*]

Rutgers University, Piscataway, New Jersey 08854, USA
(Received 11 March 2014; published 14 May 2014)

Recent experiments have demonstrated that identical material samples can charge one another after being brought into symmetric contact. The mechanism for this charging is not known. In this article, we use a simplified one-dimensional lattice model to analyze charging in the context of agitated particles. We find that the electric field from a single weakly polarized grain can feed back on itself by polarizing its neighbors, leading to an exponential growth in polarization. We show that, by incorporating partial neutralization between neighboring polarized particles, either uniform alignment of dipoles or complex charge and polarization waves can be produced. We reproduce a polarized state experimentally using identical colliding particles and raise several issues for future study.

I. INTRODUCTION

It has been known, at least since Faraday's time [1], that grains in desert sandstorms spontaneously generate multi-million volt electrical discharges. This effect has been attributed to differences in particle size or material [2]: Certainly a plausible explanation. At the same time, however, work spanning several decades in different laboratories and using different experimental systems [3–7] has shown that even identical samples of a material—including particles of the same size, shape, and composition [8]—can spontaneously break symmetry and transfer charge from one to another. Moreover, once a charge has moved from one sample to another, further contacts will transport additional charges of the same sign in the same direction, against Coulomb forces, to produce monotonically increasing charges and fields [4,6].

In the present article, we probe these findings through the examination of a simplified one-dimensional (1D) lattice of identical dielectric particles. We find that nonlinear feedback between a particle and its neighbors can cause a single infinitesimally small dipole to grow exponentially rapidly in time. We confirm experimentally that identical colliding particles do generate a self-sustaining dipole field. Additionally, if adjacent particles in the lattice model are allowed to partially neutralize one another as they might through collisional interactions, we find that new states appear in which domains of like polarization travel through the lattice. These results provide a mechanism by which collisional flows of identical grains can generate electric fields that grow and travel in complex ways.

II. ANALYSIS

We begin by considering a 1D lattice of 1000 identical particles of unit diameter, spaced a fixed distance, also one unit, apart. The dynamics of this model consists of three essential elements prescribing first, the polarization of each particle due to its neighbors, second, partial neutralization of each adjacent particle pair meant to mimic effects of collision, and third,

boundary conditions applied to the top and bottom particles. We define each element of the model here.

A. Polarization

Each particle i can host charges Q_i^{top} and Q_i^{bottom} at a vertical distance 0.375 from its center: In this manner, each particle can sustain a dipole moment $P_i = \frac{3}{4}(Q_i^{\text{top}} - Q_i^{\text{bottom}})$. Each particle feels an electric field E_i at its center due to the top and bottom charges of all of its neighbors. We calculate E_i directly using Coulomb's law, i.e., $E_i = \sum_{j \neq i} Q_j / r_{ij}^2$, where r_{ij} is the distance from the center of the ith particle to the top and bottom charges on each of the other j particles. We assume that all particles are dielectric with the same susceptibility χ_e, so that the ith particle will attain an induced dipole moment $\chi_e \cdot E_i$. This moment is added to whatever preexisting dipole may be present so that

$$P_i \rightarrow \tfrac{3}{4}\big(Q_i^{\text{top}} - Q_i^{\text{bottom}}\big) + \chi_e \cdot E_i. \quad (1)$$

Explicitly, Eq. (1) combined with charge conservation implies that the top and bottom charges become

$$\begin{aligned} Q_i^{\text{bottom}} &\rightarrow Q_i^{\text{bottom}} - \tfrac{2}{3}\chi_e \cdot E_i, \\ Q_i^{\text{top}} &\rightarrow Q_i^{\text{top}} + \tfrac{2}{3}\chi_e \cdot E_i. \end{aligned} \quad (2)$$

Thus, the polarization of a particle consists of two parts: A permanent ferroelectric polarization defined by its state following a collision and a transient paraelectric polarization slaved to the external field. We emphasize that except at the boundaries (which we discuss shortly), charge is conserved under all circumstances, however energy is not. That is, increasing polarization involves no gain or loss in net charge, however it does require an input of energy. Thus we imagine that the lattice represents an agitated bed of grains in which the energy required to polarize molecules in one grain is provided by the mechanical energy needed to draw another polarized grain closer. In this way, periodic mechanical input of energy causes grains to repeatedly approach one another, generating an increase in polarization every time step. In a previous paper, we demonstrated that identical particles can develop large charges in this way after repeated contacts in the presence of a constant external electric field [8]. In the present calculations, we use precisely the same scheme

---

*shinbrot@rutgers.edu

without applying any external field. Since the field is provided by feedback between nearby particles according to Eq. (1), in principle a particle's polarization could either increase or decrease, and indeed we will see from our simulations that both can occur.

We remark that the feedback of Eq. (1) implies an ordering to events: If particle A imparts a polarization on particle B and then particle B interacts with a third particle C, then the B-C interaction will produce a different result than if the A-B interaction had occurred later. This can be dealt with either by calculating all induced polarizations and then adding polarizations to the preexisting values at the end of each time step or by randomizing the order of interactions to eliminate systematic bias. We will compare calculations with a vibrated bed of nearly randomly [9] colliding particles, so we adopt the second alternative here.

B. Neutralization

To mimic a collisional granular flow, once per time step we allow each pair of adjacent particles, chosen in randomized order, to collide once. During each collision, we permit charges to partially neutralize with efficiency η. Explicitly,

$$Q_{i+1}^{\text{bottom}} \rightarrow \left(1 - \frac{\eta}{2}\right)Q_{i+1}^{\text{bottom}} + \frac{\eta}{2}Q_i^{\text{top}},$$

$$Q_i^{\text{top}} \rightarrow \left(1 - \frac{\eta}{2}\right)Q_i^{\text{top}} + \frac{\eta}{2}Q_{i+1}^{\text{bottom}},$$

(3)

so for $\eta = 0$, charges Q_i^{top} and Q_i^{bottom} remain unchanged after a simulated collision, and for $\eta = 100\%$, both charges revert to their average.

C. Boundary conditions

To close the description, we consider collisions on a grounded surface with a free upper boundary—as occurs, for example, in sandstorms or industrial dust clouds. So we ground the bottom of the bottom-most charge: $Q_1^{\text{bottom}} \equiv 0$, whereas the top of the topmost particle is treated like every other charge, except that it never encounters a neighbor above. As we have mentioned, charges are conserved in all collisions, except at the bottom boundary where a charge is added or removed to maintain the boundary condition $Q_1^{\text{bottom}} \equiv 0$. A final embellishment to the model is that we include image charges in the simplest possible way [10], as if the bottom surface were a perfect conductor. Simulations without image charges also were performed and do not differ noticeably from what we present here.

We make a technical clarification and then present results. Because we are ultimately interested in practical applications, we constrain the polarization to always lie within a maximum range, so $|P_i| \leq P_{\text{max}}$. This is realistic insofar as any real particle can sustain only a finite maximum charge separation beyond which dielectric breakdown will occur, but we will see momentarily that this is also computationally necessary to prevent polarizations from diverging. We choose $P_{\text{max}} = 10$, although other values have been found to produce nearly identical results.
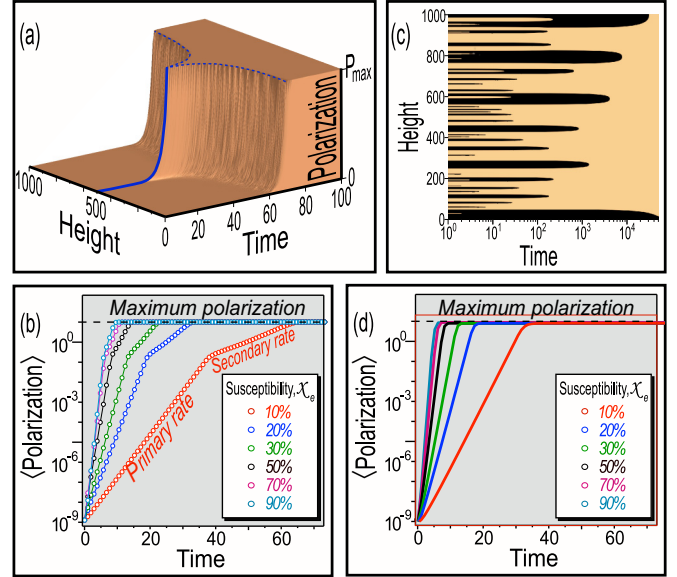

FIG. 1. (Color online) (a) Time evolution of polarizations of 1000 dielectric particles in a 1D array. Initially, the central particle is polarized by a small amount 1.5×10^{-9} computational units. (b) The mean polarization of all particles $\langle P \rangle$ grows exponentially in time at a rapid primary rate until the maximum polarization P_{max} is reached, then at a lower secondary rate. (c) Alternatively, if every particle is initially randomly polarized, multiple coarsening domains form: Light regions have $\langle P \rangle = +P_{\text{max}}$; dark regions have $\langle P \rangle = -P_{\text{max}}$. (d) In the short term, $\langle P \rangle$ grows exponentially with a faster rate than for the single particle case of (a) and (b).

As a first test of this model, we consider the simplest case without neutralization, so $\eta = 0$, and we start with all but one of 1000 particles in the zero charge and polarization state, $Q_i^{\text{top}} = Q_i^{\text{bottom}} = 0$. We initialize the center particle with a tiny polarization $P_{500} = 1.5 \times 10^{-9}$, so $Q_i^{\text{top}} = -Q_i^{\text{bottom}} = 10^{-9}$. As shown in Fig. 1(a), the central particle's polarization grows along the solid curved line until it reaches P_{max}. That particle also recruits the polarizations of its neighbors, which similarly rapidly reach P_{max}. As shown in the semilogarithmic plot of Fig. 1(b), the cumulative sum of the particles' polarizations grows exponentially with two regimes: First a steep growth as the central particle's polarization escalates and then a more moderate, but still exponential, growth as further particle polarizations are recruited. Reasonably enough, as the susceptibility increases, so does the rate at which polarization grows: This is shown in Fig. 1(d).

Apparently, in the simple case without neutralization a small initial polarization grows exponentially rapidly until the entire lattice becomes uniformly polarized. This is not mysterious: The exponential growth is a predictable consequence of the nonlinear feedback produced by adding an induced polarization $\chi_e \cdot E_i$ due to neighboring charges to every particle. Every particle obeys the same rule, so with each time step polarization must grow by a constant factor: A well-established formula for exponential growth. We emphasize that the $\eta = 0$ case produces an exponential growth in polarization, but as prescribed by Eq. (3) no transfer in charge occurs. So every particle remains charge neutral,
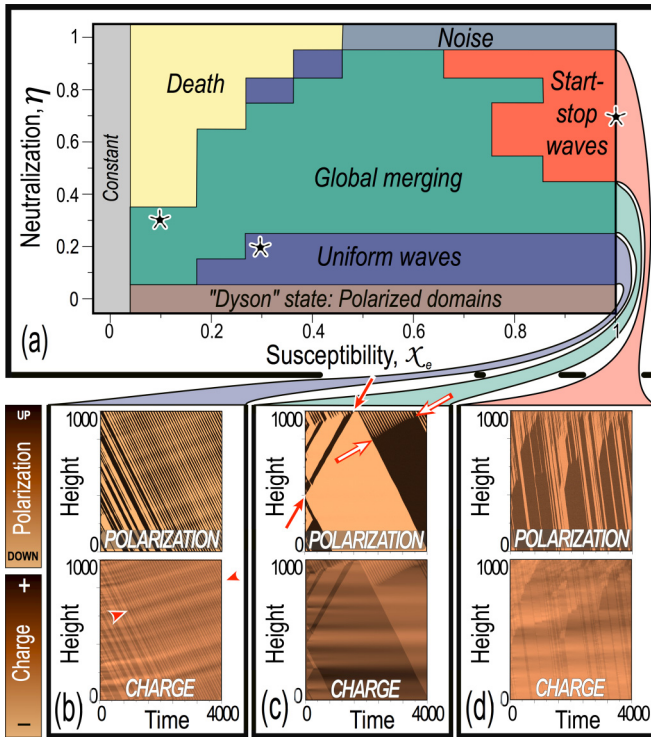
FIG. 2. (Color online) (a) Phase diagram showing distinct spatiotemporal patterns of polarization and charge dynamics. Asterisks indicate parameter values at which spatiotemporal plots beneath are taken. (b)–(d) Color-coded plots of the polarization and charge of the 1D cellular automata lattice vs time. Arrowheads in (b) identify upward motion of charge waves; solid arrows in (c) identify upward transient waves, and open arrows in (c) identify abrupt cooperative stopping of downward polarization waves discussed in the text.

whereas the polarizations of each particle in a stack rapidly approach P_{max}. We will return to this point at the conclusion of this article.

To examine a more general case, instead of beginning with a single polarized charge, we investigate the lattice dynamics if we initialize the lattice by choosing each particle's charges $Q_i^{top} = -Q_i^{bottom}$ randomly to be -1, 0, or 1. We then obtain a result as shown in Fig. 1(c) in which polarizations again grow exponentially rapidly so that adjacent regions almost immediately approach the maximum polarization $\pm P_{max}$ (shown as black and beige in the figure). Thereafter, domains coarsen until a uniformly polarized state is ultimately adopted: In our simulations of 1000 particles, this takes over 10^7 time steps.

We turn next to the case of finite neutralization, $\eta \neq 0$, as defined by Eq. (3). In this case, more complex behaviors appear, summarized in the phase diagram of Fig. 2(a). In this diagram, we identify the dynamics observed at 10% increments of susceptibility χ_e and neutralization η. For each pair of χ_e and η, the state is chosen by majority vote from three trials performed using zero charge and randomized initial polarizations for every particle as well as randomly chosen collision ordering events as described previously. Criteria for establishing what pattern is present for these votes follow: In each case, the criteria are applied after a transient period of

time steps needed to dissipate upward-moving waves (at least 500 time steps, in some cases up to 2000 time steps).

A uniformly polarized state is defined to have identical polarizations $P_i = \pm P_{max}$. This is similar to the aligned state produced by long-range ferromagnetic interactions in a 1D lattice, predicted in 1969 by Dyson [11]. In practice, as we have mentioned, we have in mind applying our lattice model to agitated granular beds, which necessarily differs from Dyson's system in several ways. First, granular beds are intrinsically nonequilibrium, so our system is not Hamiltonian. Second, dipole moments are continuous-valued rather than discrete. Third, as described in Eq. (1) we use both paraelectric and ferroelectric moments. Finally, technically Dyson's long-range interactions go as $1/r^\alpha$ for $1 < \alpha < 2$, whereas our electric field $\sim 1/r^2$ is just outside of this range. Nevertheless, in recognition of the parallel with Dyson's earlier predictions, in Fig. 2 we term $\eta = 0$ the Dyson state.

For nonzero but small neutralizations, nearly uniform downward-traveling waves of polarization $\pm P_{max}$ appear, modulated by weak and nearly orthogonal upward-traveling waves of charge. In this "uniform waves" regime shown in Fig. 2(b), widths of polarization waves vary by up to 50%, but fewer than five instances of merging of waves (discussed next) are seen. All simulations are performed using 1000 particles over 4000 time steps, and again every particle pair collides once during each time step: This duration was chosen because transient behaviors seen in the spatiotemporal plots of Fig. 2 appear to have dissipated by 4000 time steps.

As neutralization grows, increasingly irregular patterns are found. The weak modulation in downward waves [Fig. 2(b)] gives way at about $\eta = 20\%$ to waves with widths that oscillate until they merge into a uniformly polarized region, and above $\eta = 20\%$, the merging behavior travels upward in time to produce large regions of uniform polarization as shown in Fig. 2(c). Polarizations again reach $\pm P_{max}$, and we term this a "global merging" state. We note that in the middle of a large lattice of particles effects of boundaries are small, and so predictably waves travel as readily upward as, downward as indicated by solid arrows in Fig. 2(c). Both waves die at the boundaries, but the upward waves are replaced by downward waves at the free top boundary, whereas the downward waves simply end at the grounded bottom boundary. We discuss effects of boundaries shortly.

The speed of upward merging waves, identified by open arrows in Fig. 2(c), is midway between the more rapid upward transient wave speed [solid arrows in Fig. 2(c)] and the slower upward net charge speed, identified by arrowheads in Fig. 2(b). We discuss wave speeds shortly but emphasize that the root causes of these three different speeds are not understood.

At still higher η, three additional states emerge. At low χ_e, the lattice rapidly approaches zero charge and polarization irrespective of the initial condition: This is logical since particles are weakly coupled together but strongly neutralize. We term this state "death." At $\eta \approx 1$, sufficiently large χ_e's can sustain nonzero charges, but these change rapidly and show no coherent motion: We call this "noise." Finally, for large χ_e's and moderate η's, a state emerges in which both downward-traveling waves and upward-traveling merging events are seen, each traveling at different speeds. We term this state, shown in Fig. 2(d), "start-stop" waves. The polarization here remains

small, never approaching P_{max}, but coherent traveling waves are readily identifiable. We remark that the global merging state transitions gradually to start-stop waves as χ_e grows. As we have described, the lines demarking this transition are obtained from a majority vote of three trials, however, it is likely that another set of trials would result in slightly different transition lines.

Evidently there is a rich variety of patterns in this simple system, and these patterns exhibit several distinct traveling speeds. Despite its simplicity, the model involves two coupled and nonlinear fields, one for the net charge on each particle and one for its polarization, and from that perspective, perhaps the variety of behaviors is not surprising. We begin an analysis of these complex states by focusing on the simplest of the lattice dynamics, the uniform wave state.

As shown in Fig. 2(b), polarization waves tend to travel down the lattice rather than up. This asymmetry can only originate from the boundaries, for within the lattice the rules for charge dynamics are entirely symmetric—and for this reason, waves can travel both up and down until they hit the boundaries [as in the example of the solid arrows of Fig. 2(c)]. At the boundaries, symmetry is broken: As we have mentioned, the bottom boundary is grounded, whereas the top boundary is free. Without this asymmetry, for example if both boundaries are grounded, the model produces no net transport of charge or polarization.

Behavior at the bottom boundary can easily be understood. Consider the case in which the bottom-most few particles are polarized up (with plus on top). The bottom-most charge is always zero, so the bottom particle must be net positively charged to conform with the polarized-up ansatz. This will tend to induce the next particle to be more negative below and more positive above—thus, reinforcing the up-polarized state. Consequently, the bottom boundary condition strengthens the existing polarization and cannot cause the flip in polarization seen in Fig. 2(b).

Since the bottom-most charge never varies from zero, let us examine the topmost charge, whose value can change as a result of induction from the field of particles beneath. Again, consider the case of up-polarized particles. Since the topmost Nth particle is induced to be polarized up, the topmost charge Q_N^{top} will be positive, and after collision all contacting charges beneath will partially neutralize. But Q_N^{top} has no upper neighbor and so will grow monotonically due to the polarizations of particles beneath. A positive Q_N^{top} will tend to induce particles beneath to be polarized down, and since Q_N^{top} grows monotonically, at some point this topmost charge will grow until it induces the $N-1^{st}$ particle to flip signs: This occurs when the field due to Q_N^{top} exceeds P_{max}/χ_e. This begins a cascade: Once the $N-1^{st}$ particle has flipped, the particle beneath (the $N-2^{nd}$ particle) will be sandwiched between particles with opposite polarizations, and with Q_N^{top} positive, this too contributes to a flip of the $N-2^{nd}$ particle. This, of course, is not inevitable, and as shown in Fig. 2, a number of other outcomes are possible; nevertheless, this appears to be the mechanism by which symmetry is broken to produce down-moving polarization waves.

We confirm that waves emanate from the top free surface of the lattice by perturbing only the topmost charge with
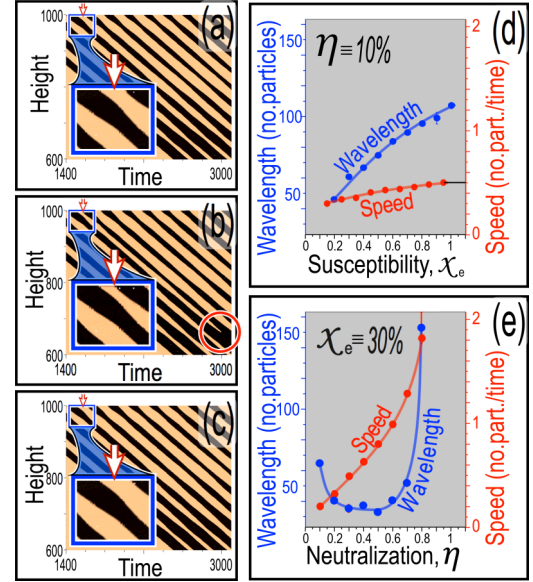

FIG. 3. (Color online) (a) Upper portion of polarization pattern from Fig. 2(b). The open arrow in the enlargement identifies time $T_o = 1475$. (b) The same pattern when a positive charge of $+10$ units is added to the topmost particle at $T_o = 1475$. Notice that this provokes a premature flip from polarization up (light) to down (dark); also note that upstream perturbation causes downstream termination of the stripe (indicated by the circle). (c) The same situation when a negative charge -10 is added at $T_o = 1475$, causing a broadening of the light stripe. (d) Wavelength and speed for χ_e for $\eta \equiv 10\%$. Note that the wavelength more than doubles as χ_e is increased, whereas the wave speed changes by about 60%. (e) Growth in η increases the speed by more than an order of magnitude but causes a nonmonotonic change in wavelength as described in text. $\chi_e \equiv 30\%$ in this panel.

parameters in the uniform wave regime $\chi_e = 0.3, \eta = 0.2$. As shown in Figs. 3(a)–3(c), artificially adding a positive charge to Q_N^{top} causes the polarizations beneath to prematurely flip, whereas subtracting the same charge causes the flip to be delayed. This effect is repeatable for charge injections at the top of the stack, however trials (not shown) in which equivalent charges are added to or subtracted from particles within the bed do not produce a change in polarization or charge waves. Apparently, the downward-moving polarization waves emanate from induced charges at the top of the stack of particles and are passively absorbed by the grounded bottom of the stack. Moreover, as identified by the circle in Fig. 3(b), pattern variations also are convected downstream by disturbances near the top of the stack—so the topmost particle affects dynamics significantly downstream as well. So the instability leading to traveling waves appears to be convective and not absolute in this system.

Evidently, the simplest dynamics, the downward-traveling polarization waves, are to some degree analytically tractable, so we continue exploiting these waves by evaluating how their wavelength λ and speed v depend on system parameters. Technically, we measure λ directly and obtain the speed using $v = \lambda/T$, where T is the measured wave period, and we evaluate λ and v during a transient period starting from random initial conditions. In this way, even if the state does not asymptotically become uniform, we can determine λ and v. Uncertainties

inevitably result over multiple measurements, and error bars are shown in Figs. 3(d)–3(e), although these are typically smaller than the plot symbols.

Beginning with Fig. 3(d), we find that λ depends strongly on χ_e at fixed η, more than doubling over the admissible range in χ_e. Wave speed changes less: by about 60%. So increasing the susceptibility or coupling between particle polarizations chiefly extends the range of collective motion (λ) and modestly increases the traveling speed of disturbances (v). Particle neutralization η, on the other hand, strongly affects traveling speed, increasing v by nearly an order of magnitude, as shown in Fig. 3(e). All of this could have been anticipated: Coupling between electric fields (χ_e) is bound to affect the range of particles affected by local charges, and the only way in which charges can be transported from one location in the lattice to another is through charge transfer from one particle to another—mediated by η.

The effect of η on the wavelength shown in Fig. 3(e) is, however, a surprise. Apparently, λ grows rapidly at either low or high η. At low η, this could have been anticipated since $\eta = 0$ must lead to the case shown in Fig. 1(c) in which the entire lattice is uniformly polarized. At high η, something else occurs: This appears to be the global merging state shown in Fig. 2(c). The cause of this and the start-stop waves state remains to be clarified in future studies. Likewise, the multiple different wave speeds identified by arrows in Figs. 2(b) and 2(c) are unexpected and merit further investigation.

III. EXPERIMENT

To test whether the predicted growth in polarization occurs in real agitated beds of identical grains, we have performed experiments as follows. It is difficult to create a truly 1D experiment since agitating grains require boundaries of some kind and boundaries unavoidably produce spurious influences such as tribocharging. To minimize potential charging at boundaries, we glued $1530 \pm 40~\mu m$ diameter glass particles inside a tall narrow (7 cm inside diameter) glass container [12], and we then filled the container to a height of 12 cm with the same glass particles and vibrated the assembly. This arrangement is not ideal—for example, the glued particles make contact only on a small area of exposed glass, whereas the free particles can make contact anywhere on their surfaces. In this context, we note that it has been known for many years that asymmetric contact between similar materials [3]—for example, between a flat surface and a round particle—can generate contact charging. Nevertheless, within the constraints of what can realistically be achieved, this configuration permits us to test whether particles do polarize as expected.

In these experiments, we first dried the particles by blowing near-zero humid air (produced by a Dryex 80 air drier) for 2 minutes prior to each experimental trial. Separate trials show humidity measured using a digital psychrometer (Extech RH300) drops to 5% relative humidity (RH) within 1 minute under these conditions. During each trial, after drying the particles we vibrate the container in a mechanical shaker at an amplitude of 2.5 ± 0.5 mm and frequency of 17 ± 3 Hz. The dry air is introduced through a plastic tube, and to prevent triboelectrification against the tube from generating spurious voltages, we removed the tube prior to each experimental trial.
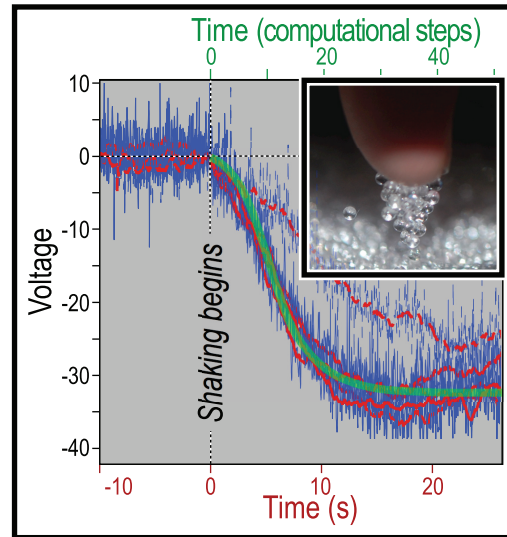

FIG. 4. (Color online) Voltage vs time from five trials in which glass beads are shaken beneath a noncontact voltage probe. The solid bold lines (red online) show running averages over 100 data points. The dashed bold curve (red online) indicates an outlier. The thick translucent line (green online) shows comparative simulation results beginning with random initial charges as in Fig. 2, here using $\eta = 0$, $\chi_e = 0.025$.

We have performed experiments at other vibrating amplitudes and frequencies; additionally we have turned the vibration on and off multiple times to establish whether material relaxation, humidity changes, or other systematic changes occur over time. All of these tests produce similar results.

Qualitatively, we find that, provided the humidity is below RH $\sim 45\%$, the particles invariably stick to a grounded intruder inserted above the vibrating bed, such as a metal rod or a finger as shown in the inset of Fig. 4 (see also Ref. [13]). Significantly, the grains stick to an intruder only so long as it is kept close to the vibrating bed: As the intruder is raised above the bed, the beads fall off. This indicates that the beads are kept in place by the presence of a strong electric field from the vibrating bed and not because of a persistent charge on the sticking beads themselves. Similarly, we have never observed beads to stick to the surface of the vibrating container, which we would expect if the beads became charged (cf. Ref. [8]). Since our experiment is at close to zero humidity, in a glass container on a wooden platform with no grounded surface or potential source of charge, it is not surprising that the particles do not acquire net charge. On the other hand, the apparent lack of charge on particles indicates that, despite the unavoidable nonideality of the experiment, tribocharging is not significant.

Quantitatively, we measure the voltage near of the vibrating bed as shown in the main plot of Fig. 4 by fixing a voltage probe above the vibrated bed and monitoring the voltage as the shaking is turned on. Measurements are taken using a Trek, Inc. (Medina, NY) model 344 voltmeter equipped with a 6000B-7C noncontact probe secured to a rod 11 ± 1 cm above the free surface of the stationary bed. At this distance, beads that bounce when the bed is vibrated never reach closer than about 2 cm from the probe. We overlay expected results

from the model described above for perfectly insulating low susceptibility particles using fit parameters $\eta = 0$, $\chi_e = 0.025$.

These experiments have been performed under a variety of conditions, including using different size and shape containers with and without glued particles. The container shape change consisted of using a convex glass vase, which has been reported to reverse or reduce granular convection; similarly, experiments were performed without glued particles because smooth boundaries reduce the extent of convection [14]. We have also performed experiments to more closely mimic our simulations in which the bottom boundary was grounded by inserting a grounded plate into the bottom of the glass container,. The data we show in Fig. 4 do not use a grounded bottom since a metal surface could tribocharge the glass particles, however all of these experiments produced similar results as those shown in Fig. 4.

We have also performed experiments using beads of different mean sizes. We find that voltages similar to those shown in Fig. 4 are obtained in those experiments, however beads significantly larger than the nominal 1530 μm diameter shown in Fig. 4 (e.g., 1800 μm beads) do not stick to an intruder, and beads significantly smaller (e.g., 630 μm beads) stick only in a monolayer. We have not evaluated charges on individual beads as a function of size, but we interpret these results to mean that by virtue of their increased mass m, larger beads have a prohibitively large Bond number Bo $= mg/F_a > 1$, where g is gravity and F_a is the cohesive electrostatic force. Smaller beads similarly produce Bo > 1 because they can sustain only a small induced polarization by virtue of their small diameters.

IV. OUTLOOK

In conclusion, a simplified 1D model for agitated insulating particles produces a rich variety of polarized and charged states that we hope may shed light on more general cases of charging of identical materials. At its simplest, when collisions are random and insulation between agitated particles is perfect, particle polarizations grow exponentially rapidly in time, resulting in a uniformly polarized state. A simple experiment using insulating particles produces results consistent with both the uniformly polarized state and its growth.

We close by identifying several avenues for future investigation that seem to be indicated by our results. First, the model predicts that if particles are permitted to transfer charge by neutralization at their points of contact, then as described in Fig. 2, the uniform state should give way to traveling waves that

become increasingly complex as the neutralization efficiency grows. However, such dynamic states have not yet been found experimentally. On the one hand, this may simply indicate that the neutralization η is very low in our experiments: A notion confirmed by the fit shown in Fig. 4 using $\eta = 0$. On the other hand, the wavelike states are a concrete prediction of the model, and future experiments engineered to more closely approximate 1D motion may reveal these states. By the same token, the 1D simplification in our model intrinsically neglects effects of particle rotation that are likely present in three-dimensional (3D) experiments, so investigations to assess how the results found in 1D change when particles rotate and interact in 3D are clearly called for.

Second, this model is restricted to the specific problem of charging of identical particles in the absence of external fields. Yet field data taken during sandstorms indicate that smaller particles tend to predominantly charge negatively [15] and that sandstorm lightning tends to occur in the presence of fields from nearby thunderstorms [16]. Expanding our model to include polydisperse particles and external fields similarly seems worth pursuing.

Third, we note that a 1D lattice of N particles with small individual polarizations p_i will cumulatively generate a total polarization $P_{\text{total}} = \sum_{i=1}^{N} p_i$, which obviously can become quite large as N grows. This leads us to speculate that voltages in excess of the Paschen breakdown limit may be achievable even in perfectly insulating particles that never individually become charged. This possibility would turn the analysis of particle charging on its head—that is, if polarization of neutral charges produces a breakdown, for example, in dry desert environments, then a breakdown could be produced in neutral grains, and charge transfer could actually follow as a result of this breakdown, rather than the breakdown occurring from particle charging as is currently assumed. This speculation seems to merit future investigation.

Finally, in all of our experiments the polarization measured is negative upwards, so that as shown in Fig. 4, shaking always produces a negative voltage above the granular bed. Possibly a difference between electron states [2,5] in freely moving beads at the top of the bed and trapped beads beneath causes this symmetry breaking, however precisely how this might occur also remains to be determined.

[1] P. F. H. Baddeley, *Whirlwinds and Dust-Storms of India*, 3 and 4 (Bell & Daldy, London, 1860).

[2] D. J. Lacks and R. M. Sankaran, J. Phys. D: Appl. Phys. **44**, 453001 (2011).

[3] J. Lowell and W. S. Truscott, J. Phys. D: Appl. Phys. **19**, 1273 (1986).

[4] T. Shinbrot, T. S. Komatsu, and Q. Zhao, Europhys. Lett. **83**, 24004 (2008).

[5] J. F. Kok and D. J. Lacks, Phys. Rev. E **79**, 051304 (2009).

[6] M. M. Apodaca, P. J. Wesson, K. J. M. Bishop, M. A. Ratner, and B. A. Grzybowski, Angew. Chem. **49**, 946 (2010).

[7] C. Cimarelli, M. A. Alatorre-Ibargüengoitia, U. Kueppers, B. Scheu, and D. B. Dingwell, Geology **42**, 79 (2013).

[8] T. Pähtz, H. J. Herrmann, and T. Shinbrot, Nat. Phys. **6**, 364 (2010).

[9] T. Shinbrot, Nature (London) **389**, 574 (1997).

[10] J. D. Jackson, *Classical Electrodynamics*, 3rd ed. (Wiley, New York, 1999), pp. 57–60.

[11] F. J. Dyson, Commun. Math. Phys. **12**, 91 (1969).

[12] cf. M. E. Möbius, B. E. Lauderdale, S. R. Nagel, and H. M. Jaeger, Nature (London) **414**, 270 (2001).

[13] See Supplemental Material at http://link.aps.org/supplemental/10.1103/PhysRevE.89.052208 for a movie of the vibrating bed with a grounded intruder.

[14] J. B. Knight, H. M. Jaeger, and S. R. Nagel, Phys. Rev. Lett. **70**, 3728 (1993).

[15] X. J. Zheng, N. Huang, and Y. H. Zhou, J. Geophys. Res.: Atmos. **108**, ACL-13 (2003).

[16] A. K. Kamra, Nature (London) **240**, 143 (1972).